

Autoresonant excitation of nonlinear beam motion in storage ringsMinghao Song^{1,2}, Linda Spentzouris,¹ Xiaobiao Huang^{2,*} and James Safranek²¹*Illinois Institute of Technology, Chicago, Illinois 60616, USA*²*SLAC National Accelerator Laboratory, Menlo Park, California 94025, USA* (Received 11 January 2022; revised 25 March 2022; accepted 27 June 2022; published 6 July 2022)

Understanding and controlling of nonlinear beam dynamics are essential to the performance of storage ring light sources. In order to measure and correct limitations due to nonlinear beam dynamics, an effective method is needed to excite the beam oscillation to large amplitudes. Autoresonance is a method that enables the control of the amplitude of a driven nonlinear oscillator by sweeping the frequency of the driver. In this study, autoresonant excitation of beam transverse oscillations in storage rings is studied. The threshold of the drive amplitude for autoresonance is theoretically obtained, for cases with or without damping. The results are in good agreement with simulations for a simple storage ring model, as well as for models of actual storage rings. Application of the theory to experimental data on the SPEAR3 storage ring also validates the results.

DOI: [10.1103/PhysRevAccelBeams.25.074001](https://doi.org/10.1103/PhysRevAccelBeams.25.074001)**I. INTRODUCTION**

Storage ring light sources continue to push for ultralow emittance to provide more powerful research tools in many physical science disciplines. Reduction of beam emittance has required more complicated lattice configurations, so it has become an increasingly bigger challenge to control the nonlinear beam dynamics. Many factors can affect the actual machine, impacting the ability to realize the design performance without correction. Poor nonlinear beam dynamics performance will generally result in a small dynamic aperture and small local momentum aperture, which in turn lead to low injection efficiency and short beam lifetime, respectively. Linear [1] and nonlinear [2–4] lattice errors need to be corrected with beam-based methods in order to reach the design performances.

Information about the nonlinear beam dynamics can be extracted from turn-by-turn beam position monitor (BPM) data, with large transverse oscillation amplitude preferred. Therefore, it is desirable to find an effective method to excite the transverse nonlinear beam motion for nonlinear beam dynamics measurement and correction. A conventional method is transversely kicking the beam with a pulsed kicker or pinger magnet. However, it suffers from fast decoherence of the kicked beam from linear and high-order chromaticities and amplitude-dependent

tune shifts [5,6]. The usable number of beam revolutions in the turn-by-turn BPM data is therefore often limited, reducing measurement precision. An alternative approach that has been widely employed in colliders [7–10] is the use of an alternating-current (ac) dipole [11]. The drive frequency of this resonant device is usually close to the natural frequency of the beam, with the frequency difference determining the driven oscillation amplitude. The application of the technique to a more nonlinear system where the natural frequency quickly changes with the oscillation amplitude is difficult as the drive frequency needs to change accordingly.

An autoresonance technique can be used to drive a nonlinear oscillator to large oscillation amplitude; this is done by applying an external excitation with swept frequency. With this technique, the beam decoherence effect is minimal. After passing through the linear resonant frequency, once the drive amplitude exceeds a certain threshold, the phase of the nonlinear oscillator continues to stay locked to the drive, and therefore the system will be driven to large amplitudes. On the contrary, if the drive amplitude is below the threshold, the phase locking does not occur and the system remains in the small amplitude state. Autoresonance has been used as an effective method of manipulating various dynamical systems; for example, atomic and molecular systems [12,13], plasma systems [14–17], fluids [18] and magnetics [19,20]. The phenomenon of autoresonance of transverse nonlinear motion was empirically employed in a past study on the SPEAR3 storage ring [21]. However, the underlying autoresonance theory was not understood and exploited. In this paper, the first comprehensive study of autoresonant excitation of storage ring beam dynamics is reported. This paper is

* xiahuang@slac.stanford.edu

Published by the American Physical Society under the terms of the [Creative Commons Attribution 4.0 International license](https://creativecommons.org/licenses/by/4.0/). Further distribution of this work must maintain attribution to the author(s) and the published article's title, journal citation, and DOI.

organized as follows: Section II describes the derivation of the autoresonance threshold theory of nonlinear beam motion in storage rings and simulations that verify the results. Section III discusses the validation of the theory with experimental results. Section IV gives the conclusion.

II. THEORY AND SIMULATION

A. Autoresonance threshold theory

The transverse beam motion in a storage ring is mainly controlled by the lattice linear optics, where bending magnets (dipoles) are used to provide a closed orbit and the arrangement of quadrupole magnets determines the transverse betatron oscillations around the closed orbit. The systematic chromatic aberration arising from quadrupole gradient errors for off-momentum particles is usually corrected with the use of sextupoles to ensure good performance of the storage ring. Consequently, the nonlinear magnetic fields of sextupoles introduce nonlinearity to the storage ring dynamics, and the equivalent octupole potential generated by the interaction of sextupoles has a larger effect on the beam motion when the system is not on a sextupole driven resonance [22]. Therefore, the actual storage ring nonlinear system can be simplified to a system as shown in Fig. 1, which consists of the linear optics and an octupole. To be specific, the horizontal beam motion is studied below, although the results are applicable to both transverse planes.

A linear oscillator can be easily driven to large oscillation amplitudes by moving the drive frequency close to the resonant frequency. For a nonlinear oscillator, as the resonant frequency varies with the amplitude, it becomes complicated. The resulting oscillation amplitude of a given drive frequency and drive amplitude depends on the state, and consequently, the history, of the oscillator. In the autoresonant excitation scheme, the beam is driven to large amplitudes by sweeping the drive tune. Depending on the sign of the detuning coefficient, the drive tune can be swept from below or above the linear betatron tune.

The autoresonant excitation of nonlinear beam dynamics in a storage ring can be studied with particle tracking simulations for the simple model shown in Fig. 1; damping

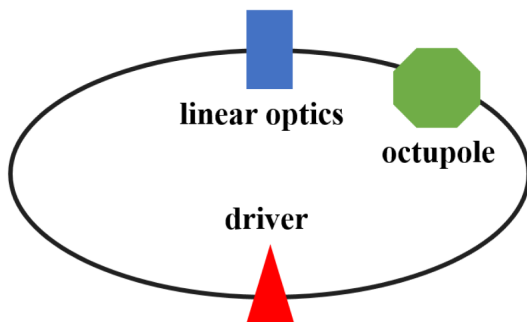


FIG. 1. Schematic of a simple nonlinear storage ring model.

effects initially are not included. In this simple model, the horizontal linear betatron tune (betatron oscillation frequency divided by the revolution frequency) is $\nu_x^{(0)} = 0.1075$. The driver and the octupole are both placed at locations where the horizontal betatron amplitude function $\beta_x = 1$ m and $\alpha_x \equiv -\frac{1}{2} \frac{d\beta_x}{ds} = 0$. The normalized octupole strength is set to $K_3(s) = 4000 \text{ m}^{-3}$, which results in a positive detuning coefficient, $\frac{d\nu_x}{dJ_x} = 470 \text{ m}^{-1}$, where $J_x = \frac{1}{2\pi} \oint x' dx = [x^2 + (\beta_x x' + \alpha_x x)^2] / (2\beta_x)$ is the horizontal action variable, and (x, x') are the position and angle coordinates. In the simulation, a particle is tracked through the elements of the ring model for many revolutions, while the drive frequency is swept upward from a starting tune of $\nu_d^{(0)} = 0.1065$ and with a sweep rate of $\frac{d\nu_d}{dn} = 1.69 \times 10^{-7}$ (tune change per turn). The tracked turn-by-turn beam position oscillation data are divided into windows of equal lengths (e.g., 256 turns) to find the amplitudes and tunes with a high-precision technique [23]. The simulation results with three different drive amplitudes are shown in Fig. 2. For the drive amplitude of $\epsilon = 0.6 \mu\text{rad}$, the drive phase and the particle oscillation phase are mismatched after the drive tune sweeps past the linear betatron tune, and hence autoresonance fails to occur. However, for the drive amplitudes of 0.8 and 1.0 μrad , the beam frequency gradually follows the drive frequency, resulting in large beam oscillation amplitudes, and the particle oscillation phase stays locked to the drive phase. Phase locking stops only when the nonlinear natural tune hits a resonance line when the beam oscillation amplitude reaches a maximum. A closer examination reveals that the bifurcation of successful or failed autoresonance, which represents the drive amplitude threshold, occurs between $\epsilon = 0.71$ and 0.72 μrad .

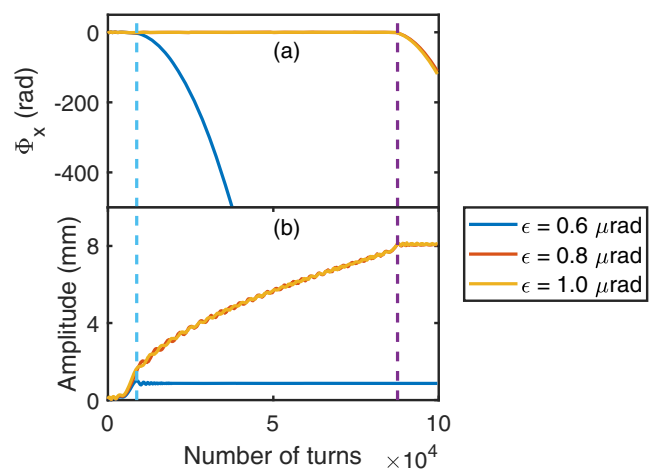


FIG. 2. (a) The difference of beam oscillation phase relative to the drive phase (phase mismatch, Φ_x), (b) beam oscillation amplitude, both as functions of the number of turns. The drive amplitudes are $\epsilon = 0.6, 0.8,$ and $1.0 \mu\text{rad}$, respectively.

In the presence of an octupole field and a resonant driver, the horizontal equation of beam motion is [24]:

$$x'' + K_x(s)x + \frac{1}{6}K_3(s)x^3 = \epsilon \sum_n \delta(s - s_d - nC) \cos \phi_d, \quad (1)$$

where the derivative is with respect to longitudinal coordinate s , $K_x(s)$ is the horizontal focusing function, s_d is the longitudinal location of the driver, n is the number of turns, and C is the circumference of the ring. The drive phase varies with the number of turns as the drive frequency is swept, $\phi_d(n) = \phi_d(0) + 2\pi[\nu_0 + \frac{1}{2}\alpha n + \frac{1}{2}an^2]$, where ν_0 is the starting tune and α is the frequency sweep rate. Note that the Dirac delta function, $\delta(\bullet)$, is used since the beam experiences a discrete kick once per revolution.

The beam motion in Eq. (1) is governed by the following Hamiltonian when expressed in the action-angle coordinates, (ϕ_x, J_x) , and with the free variable $\theta = \frac{2\pi s}{C}$ [22]:

$$H(J_x, \phi_x; \theta) = \nu_x^{(0)} J_x + \frac{1}{2} \alpha_{xx} J_x^2 + \frac{\sqrt{2}}{4\pi} \sqrt{\beta_x^d} \epsilon J_x^{\frac{1}{2}} \cos(\phi_x - \phi_d), \quad (2)$$

where the discrete drive is smoothed by expanding the drive potential in a Fourier series and dropping the fast varying terms. While the first term represents the linear motion, the second term, $\frac{1}{2} \alpha_{xx} J_x^2$, denotes the first order nonlinear betatron detuning caused by the octupole in the simple model, where $\alpha_{xx} \equiv \frac{d\nu_x}{dJ_x}$ is the nonlinear detuning of ν_x with respect to the action J_x . A similar term arises for beam motion in an actual storage ring due to the cascading effects of sextupole fields. The third term comes from the periodic drive, where β_x^d is the horizontal beta function at the driver location.

With the use of a canonical transformation to new coordinates (Φ_x, J_x) , where $\Phi_x = \phi_x - \phi_d$ is the phase mismatch, the corresponding equations of motion become

$$\frac{dJ_x}{d\theta} = 2\tilde{\epsilon} J_x^{\frac{1}{2}} \sin \Phi_x, \quad (3)$$

$$\frac{d\Phi_x}{d\theta} = \nu_x^{(0)} + \alpha_{xx} J_x - (\nu_d^{(0)} + \tilde{\alpha}\theta) + \tilde{\epsilon} J_x^{-\frac{1}{2}} \cos \Phi_x, \quad (4)$$

where we have defined the new drive amplitude and sweep rate as $\tilde{\epsilon} = \frac{\sqrt{2}}{8\pi} \sqrt{\beta_x^d} \epsilon$ and $\tilde{\alpha} = \frac{\alpha}{2\pi}$, respectively. When the variations of the natural tune and the drive tune are slow, action variable J_x can be expanded to $J_x = J_{x0} + \Delta$, with a slowly varying equilibrium action J_{x0} and a small oscillatory term Δ . With the further assumption $\Phi_x = \pi + \tilde{\Phi}_x$, with $\tilde{\Phi}_x$ small [15], J_{x0} can be found with $\nu_x^{(0)} + \alpha_{xx} J_{x0} - (\nu_d^{(0)} + \tilde{\alpha}\theta) - \tilde{\epsilon} J_{x0}^{-\frac{1}{2}} = 0$, from which we obtain $\dot{J}_{x0} \equiv \frac{dJ_{x0}}{d\theta}$ and in turn, $\dot{\Delta} = \dot{J}_x - \dot{J}_{x0}$.

For the new canonical coordinates $(\tilde{\Phi}_x, \Delta)$, the Hamiltonian is given by $\tilde{H} = \frac{1}{2} M \Delta^2 - 2\tilde{\epsilon} J_{x0}^{\frac{1}{2}} \cos \tilde{\Phi}_x + \frac{\tilde{\alpha} \tilde{\Phi}_x}{M}$, where $M = \alpha_{xx} + \tilde{\epsilon}/(2J_{x0}^{3/2})$ and the last two terms constitute a pseudopotential [14–16]. According to the new Hamiltonian, the driven nonlinear oscillation reduces to a pseudoparticle moving in a series of tilted pseudopotential wells. Phase locking is achieved when the pseudoparticle is trapped in the pseudopotential well. From the condition for the pseudopotential well to exist, $2\tilde{\epsilon} J_{x0}^{\frac{1}{2}} > \tilde{\alpha}/M$, the minimum required action for phase locking is found to be $J_{x0, \min} = (\tilde{\epsilon}/\alpha_{xx})^{2/3}$. Substituting the minimum action back into the pseudopotential well condition yields the threshold of drive amplitude for autoresonance in storage ring betatron motion,

$$\epsilon_{\text{th}} = 4\sqrt{2}\pi \left(\beta_x^d \left| \frac{d\nu_x}{dJ_x} \right| \right)^{-\frac{1}{2}} \left(\frac{|\alpha|}{6\pi} \right)^{\frac{3}{4}}. \quad (5)$$

B. Simulation of autoresonance driving

Single particle tracking with the simple storage ring model was used to test the theoretical threshold. For a series of sweep rates, the threshold drive amplitude is determined using the condition that the autoresonant fraction (i.e., the ratio of seeds that go to large oscillation amplitude) at the threshold is 0.5 [14]. Figure 3 shows a comparison of the threshold in simulation to the theoretical prediction, while the inset depicts a typical example of the determination of the drive amplitude threshold.

It is worth noting that Eq. (5) is derived for a system without damping. When damping is included, the threshold for autoresonance to occur is modified to

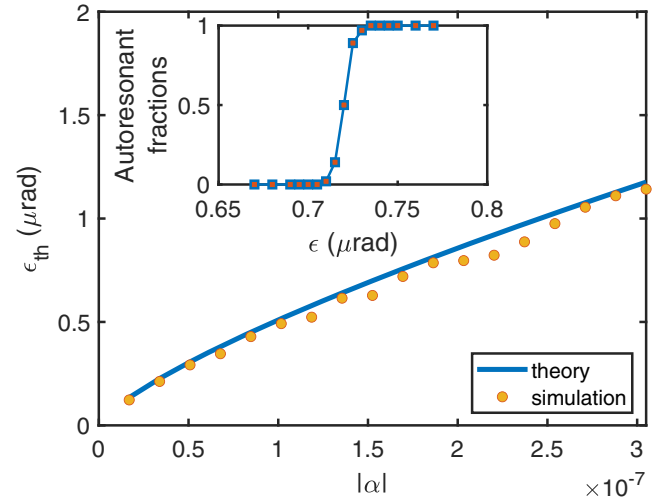


FIG. 3. Comparison of the drive amplitude threshold dependence on the sweep rate in simulation and in theory for the undamped simple model. Inset plot: autoresonant fractions versus drive amplitudes near the threshold.

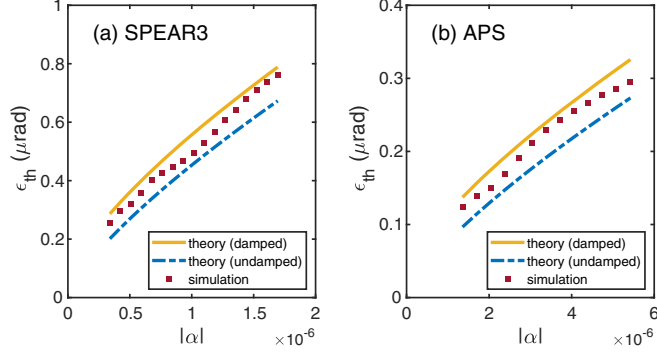


FIG. 4. Comparison of the simulated drive amplitude threshold dependence on the sweep rate to the theory for the (a) SPEAR3 and (b) APS storage rings.

$$\epsilon_{th} = 4\sqrt{2}\pi \left(\beta_x^d \left| \frac{d\nu_x}{dJ_x} \right| \right)^{-\frac{1}{2}} \left(\frac{|\alpha|}{6\pi} \right)^{\frac{3}{4}} (1 + 1.06\gamma + 0.67\gamma^2), \quad (6)$$

where γ is defined as $\gamma = \lambda_x |\alpha|^{-1/2}$, with damping decrement λ_x , and the correction factor is as found in Ref. [25]. In an actual storage ring, radiation damping is the main damping effect, for which $\lambda_x = \mathcal{J}_x \frac{U_0}{2E}$ with \mathcal{J}_x the horizontal damping partition number, U_0 the radiation energy loss per turn, and E the beam energy.

Simulation is also done with lattice models of two existing storage rings, the 3-GeV SPEAR3 storage ring at SLAC National Accelerator Laboratory and the 7-GeV Advanced Photon Source (APS) storage ring at Argonne National Laboratory (ANL). In the model, the SPEAR3 horizontal tune is $\nu_x = 0.1075$, the detuning coefficient is $\frac{d\nu_x}{dJ_x} = 3678 \text{ m}^{-1}$, and the driver device is at a location with $\beta_{xd} = 5.1 \text{ m}$. For the APS model, $\nu_x = 0.1729$, $\frac{d\nu_x}{dJ_x} = -33535 \text{ m}^{-1}$, and $\beta_{xd} = 19.5 \text{ m}$. The horizontal radiation damping decrements λ_x are 1.924×10^{-4} and 3.827×10^{-4} for the SPEAR3 and APS models, respectively. Figure 4 presents a comparison of the simulated threshold of the drive amplitude to the theory, with or without damping effects. There is a good agreement between the simulation and the theory in both storage rings.

A typical pattern of the beam oscillation amplitude under autoresonant excitation in the SPEAR3 nonlinear beam optics system as a function of the drive amplitude and the drive tune is shown in Fig. 5, where the sweep rate is fixed at 8.47×10^{-7} . It can be divided into three regions according to the drive amplitude. In region I, the beam oscillates with low amplitudes as the drive amplitudes are below the threshold. In region II, the drive amplitude is above the threshold and the beam oscillation stays in autoresonance. However, since damping is present, the maximum beam oscillation amplitude increases almost linearly with respect to the drive amplitude as the drive and damping effects reach equilibrium before the natural tune hits a resonance. In region III, the maximum oscillation

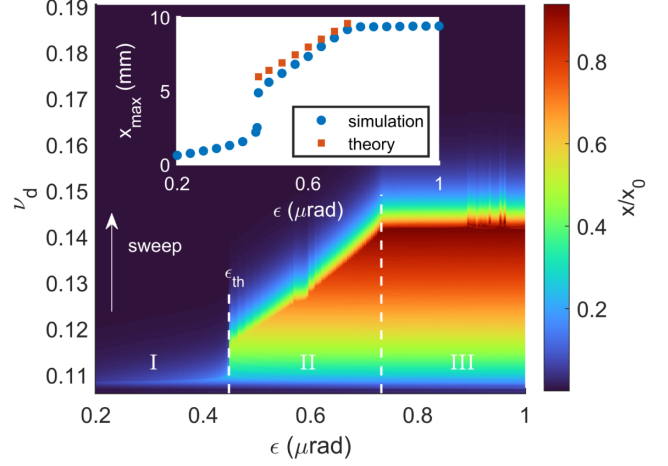


FIG. 5. Beam oscillation amplitudes (x/x_0 , with $x_0 = 10 \text{ mm}$) for the SPEAR3 model as a function of drive amplitude, ϵ , and drive tune, ν_d . The dashed line labeled by ϵ_{th} indicates the drive amplitude threshold. Inset plot: Comparison of the maximum beam oscillation amplitudes between simulation and theory in region II.

amplitude is independent of the drive amplitude since the natural tune has reached a resonance inherent to the ring lattice. When the phase is locked, the drive tune and the natural tune are equal. Considering the beam motion as a linear damped oscillator, it is easy to show that the maximum beam oscillation amplitude is given by [26]:

$$x_{\max} = \frac{\epsilon}{2\lambda_x} \sqrt{\beta_x^d \beta_x^m}, \quad (7)$$

where β_x^m is the beta function at the BPM. The maximum oscillation amplitude calculated by the equation is shown in the Fig. 5 inset plot and compared to simulations.

C. Comparison with free oscillation

In general, for an oscillator, driven oscillation differs from free oscillation in terms of frequency and amplitude. For example, in ac dipole application to hadron rings, a correction is needed for the beta function and phase advance measurements [7]. However, for autoresonance driving, the beam motion is phase locked to the drive and is thus always on resonance. Orbit data taken during the driven oscillation may be directly used for beam dynamics studies if the measured beam motion has the same characteristics as the free oscillation. For this purpose, we conducted simulation studies to compare beam motion under autoresonance driving and free oscillation.

In the simulation, the turn-by-turn orbit data during the ramping process in the autoresonant excitation are used to measure the tune and amplitude of the driven motion and are compared to the same measurement for free oscillation. Figure 6 shows the comparison of horizontal tune shift with amplitude between free oscillation and driven oscillation

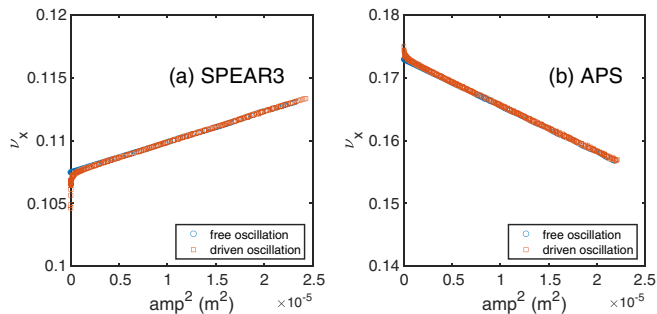


FIG. 6. Comparison of simulations of horizontal tune shift with amplitude between free oscillation and driven oscillation for the (a) SPEAR3 and (b) APS storage rings.

for the SPEAR3 and APS storage rings. Clearly, when the beam is phased locked to the drive during autoresonance, the amplitude and tune measured from the driven oscillation agree with that of the free oscillation. The excellent agreement between the two types of oscillations indicates the ramping data can be used to measure the features relevant to the nonlinear beam dynamics. Compared to the traditional method of using a single kick, the main advantage of autoresonant excitation is that a clean, sustained signal can be obtained with up to a large oscillation amplitude. This allows us to quickly and accurately measure the amplitude detuning coefficients and the resonance driving terms.

III. EXPERIMENTAL RESULTS

Autoresonant excitation has been experimentally demonstrated at SPEAR3 [21]. In the experiments, excitation was done with a stripline kicker using a signal generated by a waveform generator and amplified by an rf amplifier. The sweep time was 90 ms. By varying the starting driving frequency, the frequency span, and the output voltage, autoresonant excitation to large amplitude was realized in both the horizontal and vertical planes. In one experiment, the output voltage was scanned in ranges that covered the autoresonant thresholds for two different frequency sweep rates. The data were analyzed here to test the theoretical prediction for the drive amplitude threshold. The stripline location had $\beta_x = 10$ m and the measured detuning coefficient was 3180 m^{-1} . The frequency spans for the two cases were 60 and 80 kHz, respectively. The radiation damping decrement includes the contribution of the insertion devices. The inset plot in Fig. 7 shows the maximum beam oscillation amplitude versus the waveform generator output voltage (“Vpp”) for the case with a frequency span of 60 kHz. A pattern similar to the simulation results is observed (compare to the inset plot of Fig. 5). The x_{max} value near the threshold is obtained by fitting the linear region and is used to estimate the drive amplitude based on Eq. (7). The driving amplitude obtained from the autoresonant threshold cases is compared to the theory in Fig. 7.

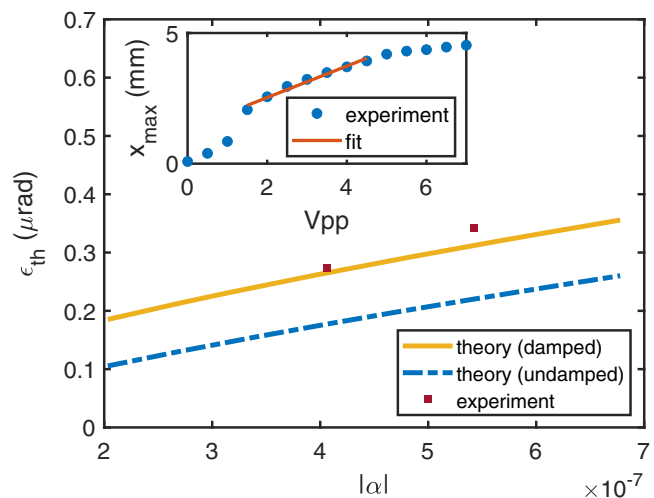


FIG. 7. Comparison of the experimental drive amplitude threshold with the theory for the SPEAR3 storage ring for two frequency sweep rates. Inset plot: Maximum beam oscillation amplitude versus waveform generator output voltage for the case with a frequency span of 60 kHz.

The prediction by the theory with damping included closely matches the experimental results.

IV. CONCLUSIONS

In this study, we have studied for the first time the application of autoresonant excitation to the transverse beam motion in storage rings. Autoresonant conditions were first realized experimentally in the SPEAR3 storage ring. The beam can be driven to large oscillation amplitudes with a weak drive amplitude under suitable conditions. Simulation with a simple storage ring model that consists of linear optics, a stripline driver, and an octupole element was able to reproduce the behavior observed in experiments. Simulations were also done with realistic SPEAR3 and APS storage ring lattice models. A systematic analysis using Hamiltonian dynamics was conducted from which the autoresonant threshold condition was obtained. The analytic result was found to be in good agreement with simulations using both the simple model and the realistic lattice models. By deriving the driving amplitude from the measured turn-by-turn beam position data, we also verified the threshold formula with experimental data from SPEAR3. Autoresonant excitation of beam motion could have important applications to the study of storage ring nonlinear beam dynamics as it can generate sustained large amplitude oscillations. This provides pronounced signals that sample the nonlinear fields in the machine, despite strong decoherence effects from large amplitude detuning or large chromaticities. Another important application of autoresonant excitation in storage rings is bunch cleaning by selectively kicking out the unwanted bunches. The results presented in this work can be used to specify the kick amplitude and tune sweep rate.

ACKNOWLEDGMENTS

This work was supported by the U.S. Department of Energy, Office of Science, Office of Basic Energy Sciences, under Contract No. DE-AC02-76SF00515.

-
- [1] J. Safranek, Experimental determination of storage ring optics using orbit response measurements, *Nucl. Instrum. Methods Phys. Res., Sect. A* **388**, 27 (1997).
 - [2] A. Franchi, R. Tomás, and F. Schmidt, Magnet strength measurement in circular accelerators from beam position monitor data, *Phys. Rev. ST Accel. Beams* **10**, 074001 (2007).
 - [3] R. Bartolini, I. P. S. Martin, J. H. Rowland, P. Kuske, and F. Schmidt, Correction of multiple nonlinear resonances in storage rings, *Phys. Rev. ST Accel. Beams* **11**, 104002 (2008).
 - [4] A. Franchi, L. Farvacque, F. Ewald, G. Le Bec, and K. B. Scheidt, First simultaneous measurement of sextupolar and octupolar resonance driving terms in a circular accelerator from turn-by-turn beam position monitor data, *Phys. Rev. ST Accel. Beams* **17**, 074001 (2014).
 - [5] R. E. Meller, A. W. Chao, J. M. Peterson, S. G. Peggs, and M. Furman, Decoherence of kicked beams, Report No. SSC-N-360, 1987.
 - [6] S. Y. Lee, Decoherence of the kicked beams II, Report No. SSCL-N-749, 1991.
 - [7] R. Miyamoto, S. E. Kopp, A. Jansson, and M. J. Syphers, Parametrization of the driven betatron oscillation, *Phys. Rev. ST Accel. Beams* **11**, 084002 (2008).
 - [8] N. Biancacci and R. Tomás, Using ac dipoles to localize sources of beam coupling impedance, *Phys. Rev. Accel. Beams* **19**, 054001 (2016).
 - [9] S. White, E. Maclean, and R. Tomás, Direct amplitude detuning measurement with ac dipole, *Phys. Rev. ST Accel. Beams* **16**, 071002 (2013).
 - [10] R. Tomás, M. Bai, R. Calaga, W. Fischer, A. Franchi, and G. Rumolo, Measurement of global and local resonance terms, *Phys. Rev. ST Accel. Beams* **8**, 024001 (2005).
 - [11] M. Bai, S. Y. Lee, J. W. Glenn, H. Huang, L. Ratner, T. Roser, M. J. Syphers, and W. van Asselt, Experimental test of coherent betatron resonance excitations, *Phys. Rev. E* **56**, 6002 (1997).
 - [12] B. Meerson and L. Friedland, Strong autoresonance excitation of Rydberg atoms: The Rydberg accelerator, *Phys. Rev. A* **41**, 5233 (1990).
 - [13] W.-K. Liu, B. Wu, and J.-M. Yuan, Nonlinear Dynamics of Chirped Pulse Excitation and Dissociation of Diatomic Molecules, *Phys. Rev. Lett.* **75**, 1292 (1995).
 - [14] J. Fajans, E. Gilson, and L. Friedland, Autoresonant (Nonstationary) Excitation of the Diocotron Mode in Non-Neutral Plasmas, *Phys. Rev. Lett.* **82**, 4444 (1999).
 - [15] J. Fajans, E. Gilson, and L. Friedland, Autoresonant (nonstationary) excitation of a collective nonlinear mode, *Phys. Plasmas* **6**, 4497 (1999).
 - [16] J. Fajans and L. Friedland, Autoresonant (nonstationary) excitation of pendulums, plutinos, plasmas, and other nonlinear oscillators, *Am. J. Phys.* **69**, 1096 (2001).
 - [17] G. B. Andresen *et al.* (ALPHA Collaboration), Autoresonant Excitation of Antiproton Plasmas, *Phys. Rev. Lett.* **106**, 025002 (2011).
 - [18] L. Friedland, Control of Kirchhoff vortices by a resonant strain, *Phys. Rev. E* **59**, 4106 (1999).
 - [19] G. Klughertz, L. Friedland, P.-A. Hervieux, and G. Manfredi, Autoresonant switching of the magnetization in single-domain nanoparticles: Two-level theory, *Phys. Rev. B* **91**, 104433 (2015).
 - [20] A. G. Shagalov and L. Friedland, Narrow autoresonant magnetization structures in finite-length ferromagnetic nanoparticles, *Phys. Rev. E* **100**, 032208 (2019).
 - [21] J. Safranek, X. Huang, J. Corbett, J. Sebek, and A. Terebilo, SPEAR3 nonlinear dynamics measurements, in *Proceedings of the 23rd Particle Accelerator Conference, Vancouver, Canada, 2009* (IEEE, Piscataway, NJ, 2009), pp. 3928–3930.
 - [22] S.-Y. Lee, *Accelerator Physics* (World Scientific Publishing Company, Singapore, 2018).
 - [23] J. Laskar, Frequency analysis for multi-dimensional systems. Global dynamics and diffusion, *Physica (Amsterdam)* **67D**, 257 (1993).
 - [24] E. Courant and H. Snyder, Theory of the alternating-gradient synchrotron, *Ann. Phys. (Paris)* **3**, 1 (1958).
 - [25] O. Naaman, J. Aumentado, L. Friedland, J. S. Wurtele, and I. Siddiqi, Phase-Locking Transition in a Chirped Superconducting Josephson Resonator, *Phys. Rev. Lett.* **101**, 117005 (2008).
 - [26] R. Bosch, Measuring betatron tunes with driven oscillations, in *Proceedings of the 23rd Particle Accelerator Conference (PAC'09), Vancouver, BC, Canada, 2009* (IEEE, Piscataway, NJ, 2009), pp. 4099–4101.